Natural product procyanidin B1 as an antitumor drug for effective therapy of colon cancer

YONGDONG LEI[1,2], XIAORONG DENG[1], ZHENGHONG ZHANG[2] and JILUAN CHEN[1]

[1]School of Food Science and Technology, Shihezi University; [2]Food Quality Supervision and Testing Center of Ministry of Agriculture, Xinjiang Academy of Agricultural and Reclamation Science, Shihezi, Xinjiang 832003, P.R. China

Abstract. Traditional chemotherapy drugs have definite antitumor mechanisms and good therapeutic efficacy; however, their poor water solubility, serious side effects and drug resistance limit their clinical application. To the best of our knowledge, the present study reported for the first time the *in vivo* and *in vitro* anticancer effects of procyanidin B1 (PCB1), a compound that is isolated from natural sources such as grape seeds, apples, peanut skin and cranberries. Cell Counting Kit-8 assay showed that PCB1 effectively decreased the number of viable HCT-116 cells compared with cells treated with the small molecule cytotoxic drug doxorubicin. Quantitative PCR and apoptosis analysis, Cell cycle analysis, and WB analysis) of the molecular mechanism showed that PCB1 induced cell apoptosis and cell cycle arrest in S phase by increasing expression of pro-apoptosis protein caspase-3 and BAX and decreasing expression of anti-apoptosis protein Bcl-2. The efficient antitumor activity of PCB1 was demonstrated through *in vivo* experiments on a xenograft mouse model, demonstrating that PCB1 significantly suppressed tumor growth. The present study suggested that PCB1 represents a novel class of plant-based compounds isolated from natural sources that can be applied as an anticancer drug.

Introduction

Colon cancer is a malignant tumor of the digestive tract that occurs in the colon mucosa (1,2). Diet, environment and genetic factors affect the pathogenesis of colon cancer (3,4). Currently, colon cancer is primarily treated using surgery; however, most patients are already in the advanced stage when they are diagnosed because the disease has no clear symptoms in the early stage (5,6). Chemotherapy and radiation therapy are key strategies for antitumor therapy when the tumor progresses to mid- and late-stage (7-10). However, the ionizing radiation associated with radiation therapy causes severe side effects such as loss of appetite, fatigue, headache, dizziness, nausea, vomiting and bone marrow suppression (11-14). The existing chemotherapeutic drugs, such as sorafenib, doxorubicin, 5-fluorouracil and cisplatin, have definite antitumor mechanisms and effects, but shortcomings such as low cytotoxic selectivity, poor water solubility, serious side effects, low bioavailability and drug resistance limit their application (15-18). Therefore, it is necessary to explore novel drugs with efficient anticancer effects and low acute and long-term toxicity to improve the disease-free survival time and decrease the postoperative recurrence rate.

Several plant-based compounds have been shown to be potent anticancer drugs or chemosensitizers or to reverse drug resistance in different tumors (19-22). Compared with small molecule cytotoxic drugs, plant-based compounds show advantages such as multi-targeting, low toxicity, precise function and easy synthesis. Procyanidins (PCs) are a class of natural polyphenolic compounds found in a variety of plants, such as grape seeds, apples, peanut skin and cranberries (23-25). Owing to the strong antioxidant capacity and free radical scavenging ability, PC exhibits a wide range of applications in protecting cardiovascular circulation, anti-inflammatory and immunity enhancement (26-28). In addition, acute and long-term toxicity evaluation showed excellent biocompatibility, which is the basis for its biomedical applications (23). Currently, the application of PC in biomedicine has been extended to tumor therapy but studies on the antitumor effects of PC are limited to their total extracts (29-31). To the best of our knowledge, no anticancer activity evaluation of PC with specific polymerization degree and structural characteristics has been reported so far.

Materials and methods

Cell culture. Human colon carcinoma cell line HCT-116, colorectal adenocarcinoma epithelial cell line DLD-1 and colon cancer cell line SW620 were purchased from the Cell Bank of Type Culture Collection of Chinese Academy of Sciences (Shanghai, China) and cultured in a 5% CO_2 incubator at 37˚C. HCT-116 cells were cultured in McCoy's 5A supplemented with 10% fetal bovine serum (FBS), 1% streptomycin and penicillin (all Gibco; Thermo Fisher Scientific, Inc.). DLD-1

Correspondence to: Professor Jiluan Chen, School of Food Science and Technology, Shihezi University, 221 North Fourth Road, Shihezi, Xinjiang 832003, P.R. China
E-mail: 1134341580@qq.com

cells were cultured in RPMI-1640 (Gibco) supplemented with 10% FBS and 1% streptomycin and penicillin. SW620 cells were cultured in Leibovitz's L-15 (Gibco) supplemented with 10% FBS and 1% streptomycin and penicillin. For the CCK-8, apoptosis and cell cycle assay, HCT-116, DLD-1 and SW620 cells were treated with PCB1 (purity >95%, Shanghai Yuanye Biotechnology Co. LTD) (0, 6, 12, 25, 50, and 100 μg/ml) or DOX (100 nM) (MCE) in a serum-free culture medium at 37°C for 24, 48, or 72 h.

CCK-8 assay. CCK-8 assay was used to assess viability of HCT-116, DLD-1 and SW620 cells incubated with PCB1 or DOX. HCT-116, DLD-1 or SW620 cells were seeded into a 96-well plate at a density of 5×10^3 cells/well and incubated overnight at 37°C. Subsequently, culture medium was replaced with that containing PCB1 or DOX. After incubation at 37°C for 24, 48 and 72 h, 10 μl of CCK-8 reagent was added to each well and incubated with cells for 2 h. Then the absorbance of cells at 450 nm was measured with a microplate reader.

Apoptosis assay. Apoptosis assay was performed to measure early or late apoptotic HCT-116 cells following treatment with PCB1 or DOX. Briefly, HCT-116 cells were first seeded into 6-well plates at the density of 2×10^5 cells per well and incubated overnight at 37°C. Following treatment with PCB1 or DOX for 48 h at 37°C, HCT-116 cells were washed twice with PBS and re-suspended in binding buffer at a density of 1×10^6 cells/ml. HCT-116 cells (100 μl), Annexin V-FITC (5 μl) and PI (5 μl) were mixed and transferred to a tube for incubation at 37°C for 15 min. The binding buffer (400 μl) was added to the stained HCT-116 cells, which were analyzed using a flow cytometer (BD FACS Calibur; BD Biosciences) and FlowJo 10.8.1 (BD Biosciences).

Cell cycle analysis. Cell Cycle Assay Kit, DOJINDO) was used to analyze the effect of PCB1 on the cell cycle. Briefly, HCT-116 cells first seeded into a 6-well plate at the density of 2×10^5 cells per well and incubated overnight at 37°C. After treatment with PCB1 or DOX for 48 h at 37°C, HCT-116 cells were added to PBS and fixed in cold ethanol (70%, 4°C) for 4 h. The mixed solution was centrifugated at 37°C (500 x g, 5 min) for removing ethanol and then added to DNA staining solution (500 μl). Following incubation at 37°C for 30 min, HCT-116 cells were analyzed using a flow cytometer (BD FACS Calibur; BD Biosciences). The data were analyzed by FlowJo 10.8.1 (BD Biosciences).

Reverse transcription-quotative (RT-q)PCR. Following treatment with PCB1 or DOX at 37°C for 48 h, total RNA was extracted from HCT-116 cells using TRIzol™ (Thermo Fisher Scientific, Inc.; Invitrogen). Total RNA was reverse-transcribed into cDNA (1 μg) using the PrimeScript™ RT Reagent kit (Takara Bio, Inc.), according to the manufacturer's protocol. qPCR was performed using SYBR®-Green Premix Ex Taq™ (Takara Bio, Inc.) on a QuantStudio™ 5 Real-Time PCR Detection System (Applied Biosystems; Thermo Fisher Scientific, Inc.), according to the manufacturer's protocol. The following primer pairs were used for qPCR: Caspase-3 forward, 5'-GGTGCTATTGTGAGGCGGTT-3' and reverse, 5'-TGAGAATGGGGGGAAGAGGCA-3'; Ki67 forward, 5'-ATGGAGAGGTGGCCAAGAAC-3' and reverse,

5'-TGTGTGGTCTGTGTGAGCTG-3'; Bcl-2 forward, 5'-CTTTGAGTTCGGTGGGGTCA-3' and reverse, 5'-GGG CCGTACAGTTCCACAAA-3'; Bax forward, 5'-CCCGAG AGGTCTTTTTCCGAG-3' and reverse, 5'-CCAGCCCAT GATGGTTCTGAT-3' and β-actin forward 5'-GGACTTCGA GCAAGAGATGG-3' and reverse, 5'-AGCACTGTGTTG GCGTACAG-3'. The mRNA levels were quantified using the $2^{-\Delta\Delta Cq}$ method (32) and normalized to the internal reference gene β-actin.

Western blotting. HCT-116 cells were seeded into a 6-well plate at a density of 2×10^5 cells per well and incubated overnight at 37°C. After treatment with PCB1 at 37°C for 24 h, HCT-116 cells were lysed in cold RIPA lysis and extraction buffer (cat. no. 89900; Thermo Fisher Scientific, Inc.) at 4°C for 30 min. The protein extract was centrifugated at 12,000 x g for 5 min at room temperature to collect the cell lysate. Total protein was quantified using the BCA Protein Detection kit (cat. no. 23227; Thermo Fisher Scientific, Inc.) and 20 μg protein/lane was separated by SDS-PAGE on 10 and 12% gels. The separated proteins were transferred onto a PVDF membrane using a western blot system (Bio-Rad Laboratories, Inc.). PVDF membranes were blocked with 5% skimmed milk powder for 1 h at 4°C and then incubated with primary antibodies at 4°C overnight. The following antibodies were used at a dilution of 1:1,000: Anti-cleaved-Caspase-3 (cat. no. 9661T; Cell Signaling Technology, Inc.), anti-Ki67 (cat. no. ab16667; Abcam), anti-Bax (cat. no. 14796S; Cell Signaling Technology, Inc.) and anti-Bcl2 (cat. no. ab59348; Abcam). The PVDF membranes were washed three times with TBST (8.8 g NaCl + 20 ml of Tris-HCL (1 M) + 0.5 ml of Tween 20) and then incubated with secondary antibodies for 1 h at room temperature as follows: Anti-rabbit IgG (1:5,000; cat. no. 7074; Cell Signaling Technology, Inc.) or anti-mouse IgG, horseradish peroxidase-linked antibody (1:5,000; cat. no. 7076; Cell Signaling Technology, Inc.). After incubation, the membranes were washed, added with ECL reagent (SuperSignal West Femto, Thermo Scientific) and observed by enhanced chemiluminescent detection systems (chemiscope6100, Shanghai Qinxiang Scientific Instrument Co., LTD) and analyzed by ChemiScope Analysis software (Shanghai Qinxiang Scientific Instrument Co., LTD).

Solid tumor treatment. A total of 25 female BALB/c nude mice (age, 5 weeks, weight, ~20 g) were purchased from Slack Experimental Animal Center (Shanghai, China). All animal experiments were approved by the Biology Ethics Committee of Shihezi University (approval no. A2022-046). All mice were housed in an animal facility under constant environmental conditions (room temperature, 22±1°C, relative humidity, 40-70% and a 12 h light-dark cycle) and allowed free access to autoclaved water and irradiated food HCT-116 tumor models were established by subcutaneous injection of 6×10^6 cells into the right shoulder of nude mice. The mice were randomly divided into five groups (n=5/group) after the tumor volume reached ~50 mm^3 as follows: Control (PBS), PCB1 (20 mg/kg), PCB1 (40 mg/kg), PCB1 (60 mg/kg) and DOX (5 mg/kg) groups. The mice received intragastric PCB1 or DOX every other day via gavage. The tumor size was measured every day and calculated using as follows: (Length x width^2)/2. Animals were euthanized when the individual tumor volume
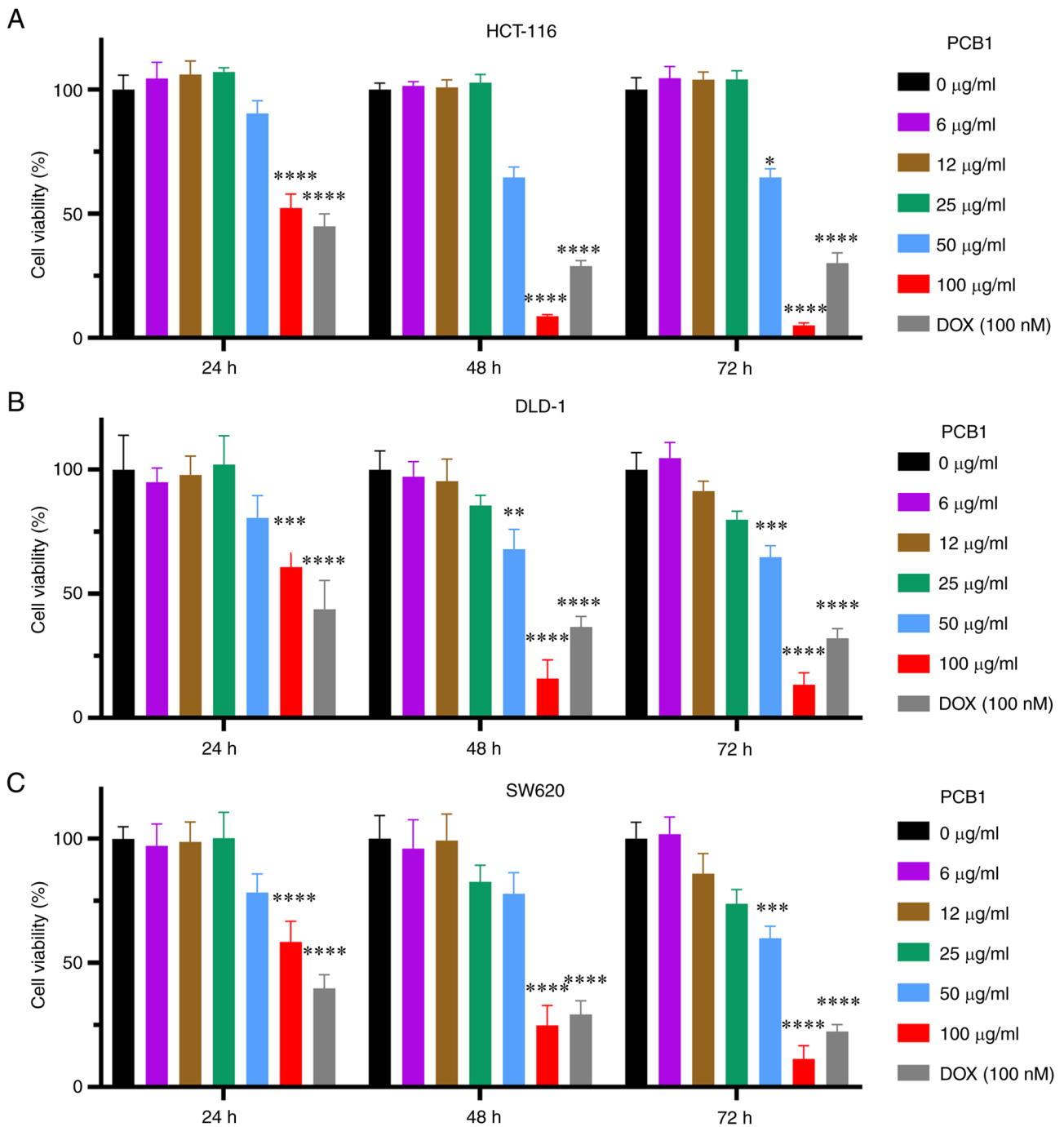
Figure 1. *In vivo* anticancer activity of PCB1. Anticancer activity of PCB1 in (A) HCT-116, (B) DLD-1 and (C) SW620 cells was evaluated using Cell Counting Kit-8 assay. DOX (10 nM) was used as the positive control. PCB1, procyanidin B1; DOX, doxorubicin. *P<0.05, **P<0.01, ***P<0.002, and ****P<0.001, which was compared with 0 μg/ml.

reached 1000 mm³. No animals were sacrificed according to the endpoints before the end of the experiment. After 18 days of administration, the experiment was terminated. The mice were euthanized after being photographed. Euthanasia was performed using 5% isoflurane inhalation followed by cervical dislocation. The tumors were collected, photographed and weighed to evaluate the anticancer activity of PCB1.

Statistical analysis. Data are expressed as the mean ± standard deviation and analyzed by Graphpad Prism 8.0 (GraphPad Software). To ensure the accuracy of the experiments, at least three replicates were performed. When variances were homogeneous, the statistical analysis was performed through one-way ANOVA. If not, the data were analyzed using the Kruskal-Wallis non-parametric test. If there was significant difference, the data were analyzed using Dunnett's post hoc test.

Results

Viability of HCT-116 cells incubated with PCB1 using CCK-8 assay. The concentration-dependent cytotoxicity of PCB1 is reported in Fig. 1A. PCB1 decreased the number of
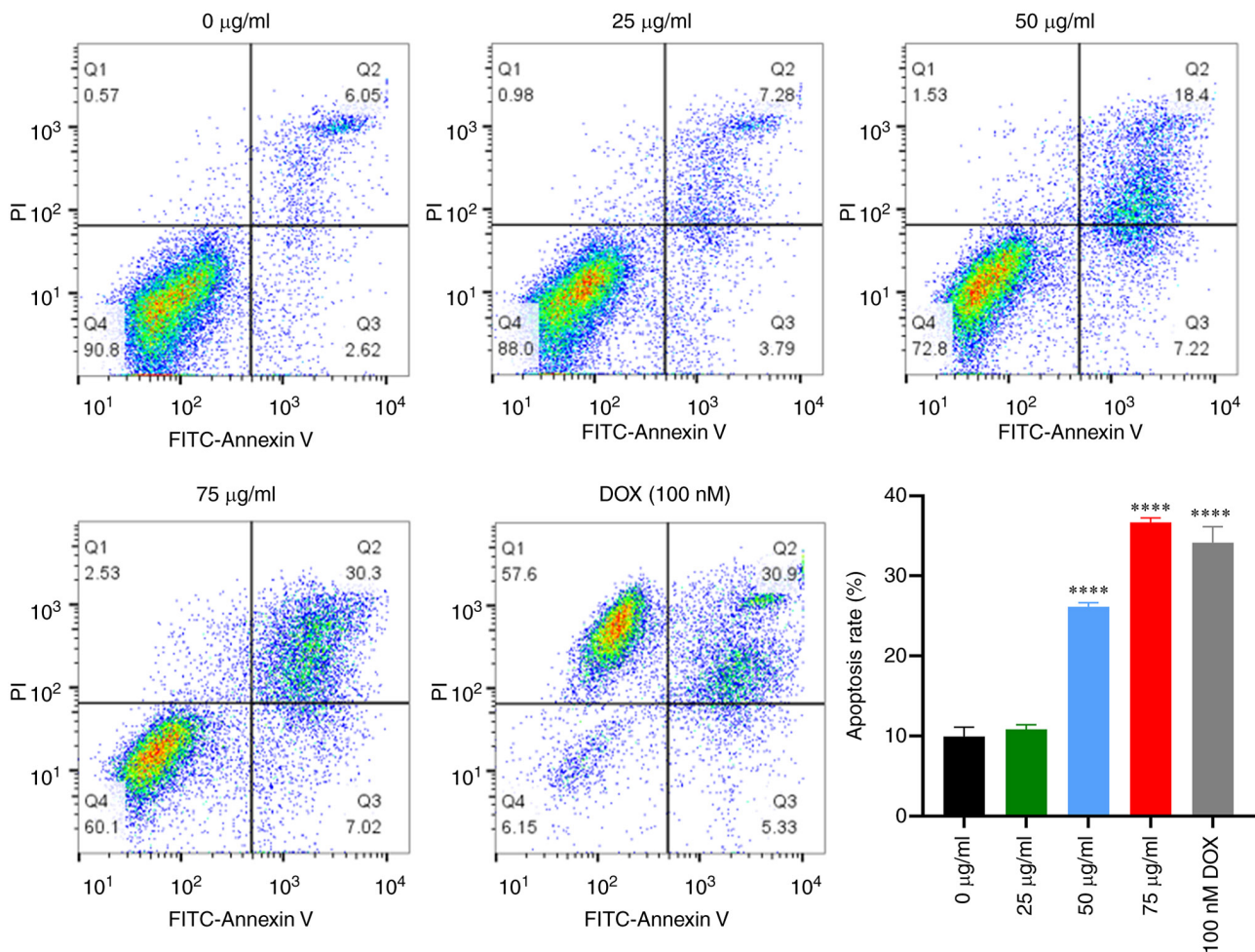
Figure 2. Effect of PCB1 on cell apoptosis. Apoptosis analysis of HCT-116 cells treated with PCB1. DOX (100 nM) was utilized as the positive control. PCB1, procyanidin B1; DOX, doxorubicin. ****P<0.001, which was compared with 0 μg/ml.

live HCT-116 cells; 100 μg/ml PCB1 induced a 52.3±5.0% decrease in live cells after treating for 24 h. By contrast, viability of HCT-116 cells incubated with PCB1 for 48 or 72 h was decreased to 8.7±0.5 and 5.0±0.9%, respectively, which was lower than that of DOX at the same incubation length (28.9±2.2 and 30.1±4.1% for 48 and 72 h, respectively). Moreover, a significant decrease in cell viability was observed for DLD-1 and SW620 cells following incubation with PCB1, with 100 μg/ml PCB1 showing the greatest effect on cancer cells (Fig. 1B and C). DOX was chosen as a positive control because it is a widely used and studied anticancer drug (33-35).

Apoptosis analysis. The mechanism of cell death induced by PCB1 was investigated using flow cytometry. A significant increase in apoptotic HCT-116 cells was found following treatment with PCB1 or DOX for 48 h. Moreover, apoptosis of HCT-116 cells induced by PCB1 was concentration-dependent (Fig. 2). Specifically, the apoptosis rate of HCT-116 cells at 48 h increased from 11.07 to 37.32% as the concentration of PCB1 increased. Furthermore, levels of apoptotic HCT-116 cells following incubation with PCB1 for 48 h were higher than in the DOX group (37.32 vs. 36.23%), indicating that PCB1 efficiently induced cell apoptosis.

Cell cycle analysis. Given the cell apoptosis induced by PCB1, cell cycle analysis was performed to verify if PCB1 caused cell cycle arrest. The proportion of HCT-116 cells in each phase was measured following treatment for 48 h with either PCB1 or DOX using a flow cytometer. The accumulation of HCT-116 cells treated with DOX in S phase and G_2/M phase was accompanied by reduction in G_0/G_1, demonstrating the DOX-induced S phase and G_2/M phase arrest (Fig. 3). By contrast, the proportion of HCT-116 cells in S phase following treatment with PCB1 was increased compared with that in the control group, while that in G_0/G_1 phase was significantly decreased. Furthermore, the proportion of cells in the S phase increased in a concentration-dependent behavior, suggesting HCT-116 cell cycle progression was arrested in S phase by PCB1, thereby inducing cell apoptosis.

RT-qPCR analysis and western blotting. Considering that cell apoptosis and cell cycle arrest were induced by PCB1, RT-qPCR and western blotting were performed to investigate the possible apoptotic pathways. Following treatment with PCB1, the PCB1 group (75 μg/ml) showed an increase in mRNA expression levels of pro-apoptosis proteins caspase-3 and BAX compared with those in the control group. By contrast, the mRNA expression of anti-apoptosis protein Bcl-2
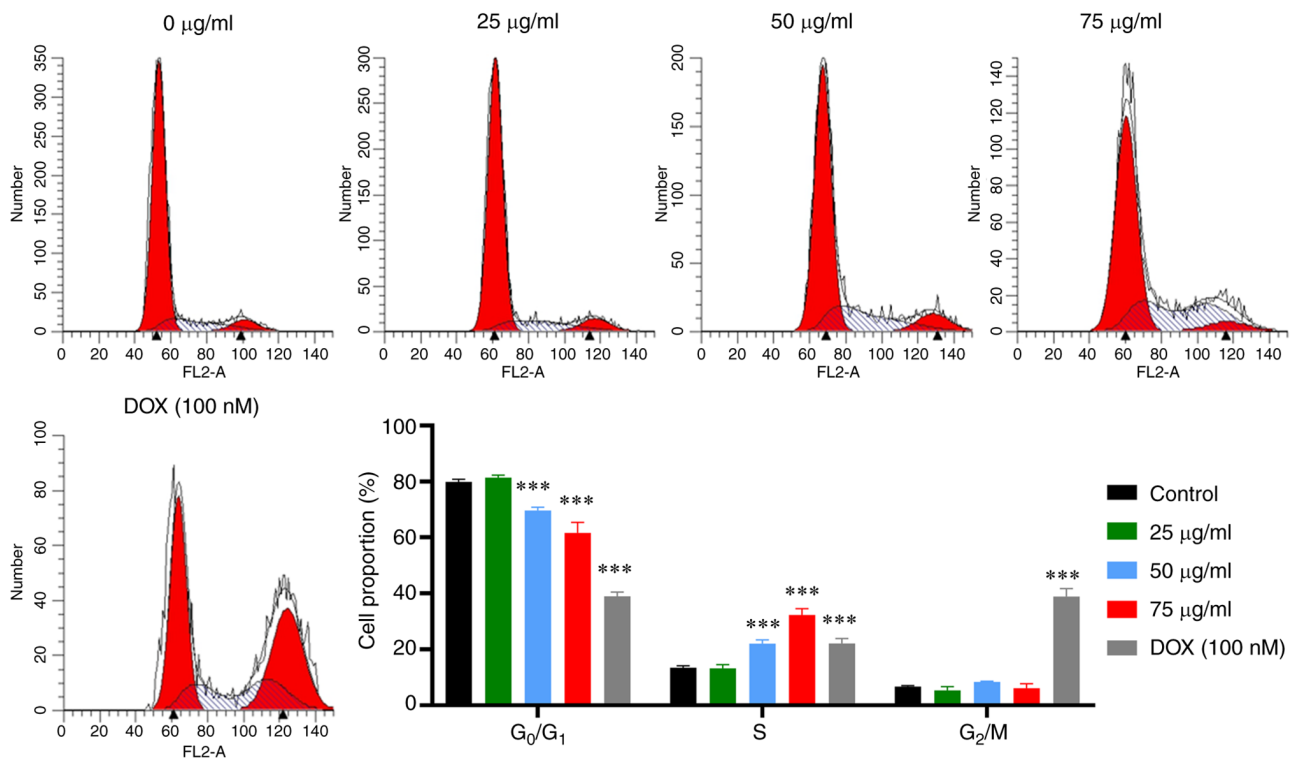
Figure 3. Effect of PCB1 on cell cycle. Cell cycle analysis of HCT-116 cells treated with PCB1. DOX (100 nM) was utilized as the positive control. PCB1, procyanidin B1; DOX, doxorubicin. ***$P<0.002$, which was compared with 0 μg/ml.

in HCT-116 cells treated with PCB1 significantly decreased as the concentration of PCB1 increased (Fig. 4).

In addition, the protein expression of caspase-3 and BAX in HCT-116, DLD-1 and SW620 cells increased compared with the control group, while that of Bcl-2 was notably decreased (Fig. 5). These results demonstrated that the PCB1 treatment induced caspase-associated apoptosis pathway. Moreover, mRNA and protein expression levels of Ki-67 were also decreased in the PCB1 group compared with those in the untreated group, confirming that PCB1 inhibited cell proliferation.

In vivo therapeutic efficacy of PCB1. The efficient anticancer and apoptotic activity of PCB1 at the cellular level suggested that PCB1 may be potentially applied in clinical practice. Therefore, the *in vivo* therapeutic efficacy of PCB1 on an HCT-116 xenograft tumor model induced via intragastric administration was investigated. Representative photographs, tumor volume and weight and body weight of mice treated with PBS, PCB1 (25 μg/ml, 20 mg/kg), PCB1 (50 μg/ml, 40 mg/kg), PCB1 (75 μg/ml, 60 mg/kg) and DOX (100 nM, 5 mg/kg) are presented in Fig. 6. No inhibitory effect on the tumor growth was observed in the control group (Fig. 6D). By contrast, the tumor volume in the low-dose (20 mg/kg) and mid-dose (40 mg/kg) PCB1 groups were significantly lower than that in the control group, suggesting that PCB1 had an efficient antitumor activity in this model. Moreover, the tumor growth inhibition in the high-dose (60 mg/kg) PCB1 group was comparable with the DOX (100 nM) group (Fig. 6A and B) In addition, the tumor weight in the high-dose PCB1 (60 mg/kg) and DOX groups were significantly lower than that in the control group (Fig. 6C), further confirming

the antitumor ability of PCB1. No significant change in body weight in each group was observed (Fig. 6E), suggesting good biocompatibility and undetectable off-target toxicity of PCB1.

Discussion

Existing chemotherapeutic drugs, such as 5-fluorouracil, oxaliplatin and capecitabine, for the treatment of colon cancer, have definite antitumor mechanisms and effects but also shortcomings, such as low cytotoxicity selectivity, poor water solubility, serious side effects, low bioavailability and drug resistance, that limit their clinical application (36-38). By contrast, the present study showed that PCB1 may be a potential novel anticancer agent that originates from natural polyphenolic compounds and possesses good biocompatibility. To the best of our knowledge, although the application of PC in biomedicine has been extended to tumor therapy, studies on the antitumor effects of PC are limited to their full extracts (29-31); moreover, no anticancer activity of PC with specific polymerization degree and structural characteristics has been reported.

CCK-8 assay revealed that PCB1 effectively decreased the number of viable HCT-116 cells compared with the small-molecule cytotoxic drug doxorubicin (DOX). Moreover, the expression levels of several important genes are assessed to establish the anticancer mechanism of PCB1 as a potential chemotherapy drug. Further analysis demonstrated that PCB1 blocked the cell cycle of HCT-116 cells in the S phase by decreasing the expression of Ki67 and Bcl-2 and increasing the expression of Caspase-3 and BAX. *In vivo* experiments on a xenograft mouse model indicated that PCB1 significantly inhibited tumor growth, comparably to the effect of DOX.
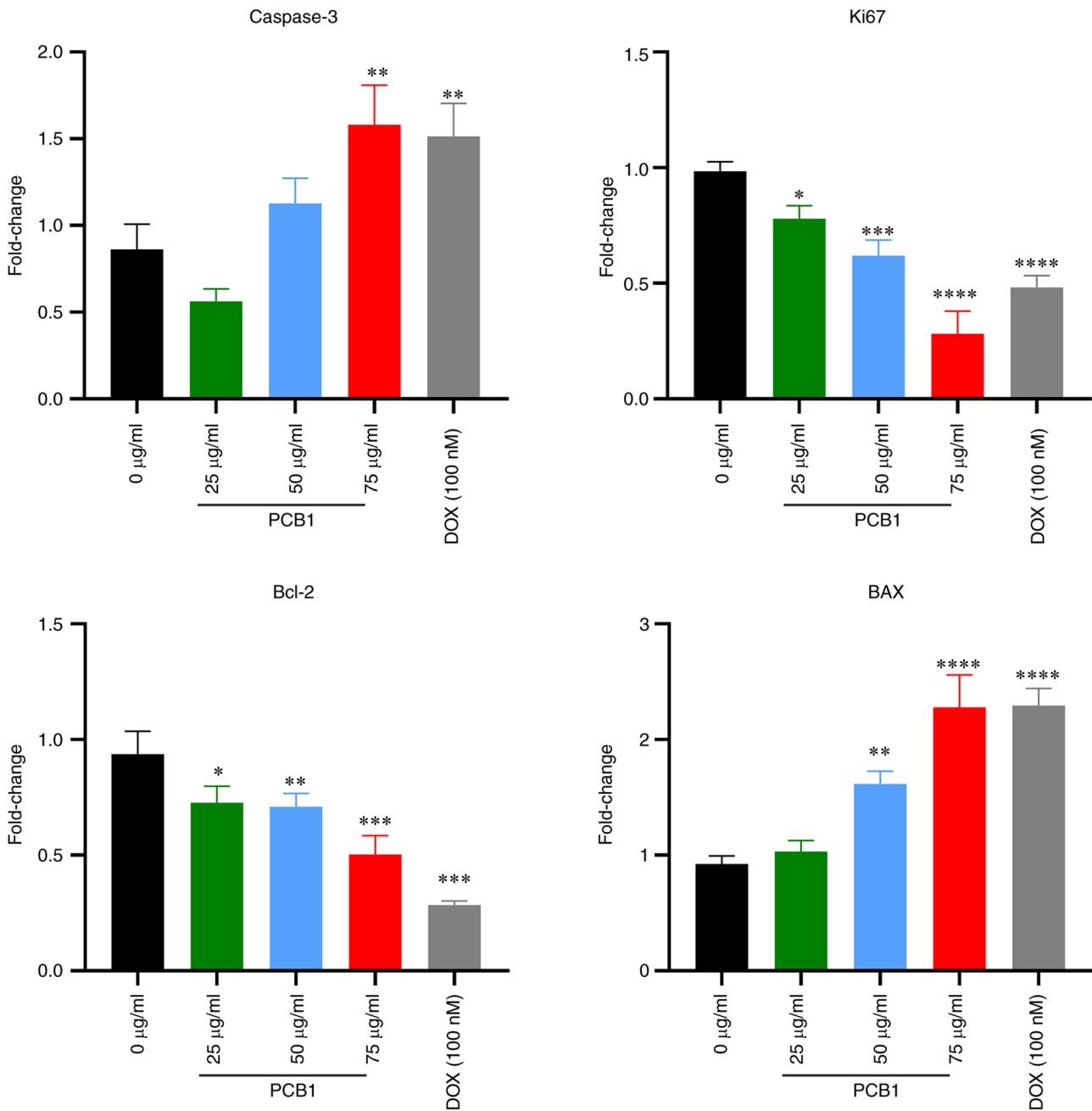
Figure 4. mRNA expression levels in cells treated with PCB1. mRNA expression levels of Caspase-3, Ki67, Bcl-2, and BAX in HCT-116 cells treated with PCB1. DOX (100 nM) was used as the positive control. PCB1, procyanidin B1; DOX, doxorubicin. *P<0.05, **P<0.01, ***P<0.002, and ****P<0.001, which was compared with 0 μg/ml.

In the present study, the increased proportion of cells in S phase suggested that PCB1 arrested HCT-116 cell cycle progression, thereby inducing cell apoptosis. Mammalian cells mainly possess two major apoptotic pathways including the death-receptor and the mitochondrial pathways. Considering that the two pathways converge at the caspase-3 protein, we thus detected the expression of caspase-3 in the mRNA and protein levels to investigate the apoptotic pathways. RT-qPCR and western blot analysis further indicated that PCB1 increased the protein and mRNA levels of caspase-3 and BAX and decreased those of Bcl-2. Although RT-qPCR and western blot experiments have suggested that PCB1 induces cell apoptotic, the potential anticancer mechanism of PCB1 has

not been investigated. More experiments will be performed in future to investigate the anticancer mechanism of PCB1, such as the comet assay, topoisomerase inhibition assay and lactate dehydrogenase assay. In addition, the potential anticancer activity of PCB1 against non-transformed cell lines would be carefully evaluated in the future. Unlike DOX (34), the plant-based compound PCB1 does not induce notable damage to normal tissues and important organs. However, the *in vivo* therapeutic effect of PCB1 was limited. Therefore, further studies should investigate the combined therapeutic effect of PCB1 and commonly used first-line chemotherapy drugs. Although the present results suggested PCB1 as a potential chemotherapy drug to inhibit tumor growth, the current study
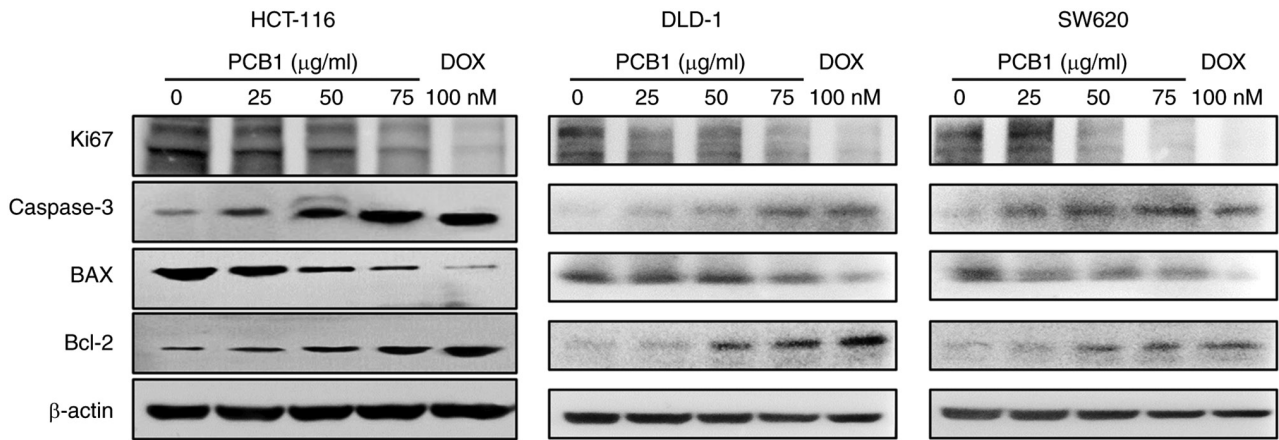
Figure 5. Protein expression levels. The protein expression levels of Caspase-3, Ki67, Bcl-2, and BAX in HCT-116, DLD-1, or SW620 cells treated with PCB1. DOX (100 nM) was utilized as the positive control. PCB1, procyanidin B1; DOX, doxorubicin.
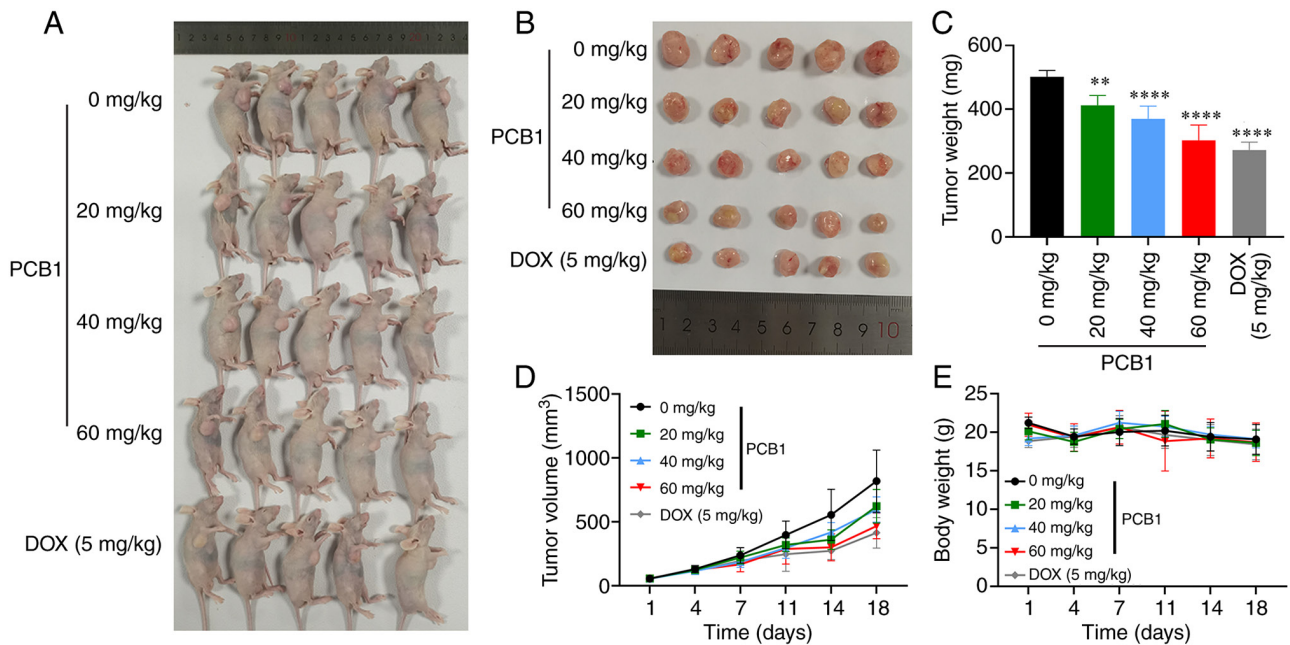

Figure 6. Effect of PCB1 on tumor growth in xenograft mouse model. Representative photographs of (A) mice and (B) excised tumors following treatment with PCB1. Tumor (C) volume and (D) weight and (E) body weight curves after treatment with PCB1. DOX (5 mg/kg) was utilized as the positive control. PCB1, procyanidin B1; DOX, doxorubicin. **$P<0.01$ and ****$P<0.001$, which was compared with 0 mg/kg.

was not comprehensive and the anticancer mechanism of PCB1 was not investigated at the cellular and molecular levels. Investigation of the anticancer mechanism of PCB1 compared with other anticancer drugs should be performed in the future. In addition, the *in vivo* long-term toxicity of PCB1 should be evaluated in the future.

Acknowledgements

Availability of data and materials

The datasets used and/or analyzed during the current study are available from the corresponding author on reasonable request.

Authors' contributions

JC designed the study. YL, XD and ZZ collected and analyzed data. YL wrote the manuscript. All authors have read and approved the final manuscript. YL and JC confirm the authenticity of all the raw data.

Ethics approval and consent to participate

All animal experiments were approved by the Biology Ethics Committee of Shihezi University (approval no. A2022-046).

Patient consent for publication

Not applicable.

Competing interests

The authors declare that they have no competing interests.

References

1. Liu F, Wang XD and Du SY: Production of gold/silver doped carbon nanocomposites for effective photothermal therapy of colon cancer. Sci Rep 10: 7618, 2020.
2. Wang X, Zhong X, Lei H, Geng Y, Zhao Q, Gong F, Yang Z, Dong Z, Liu Z and Cheng L: Hollow Cu2Se nanozymes for tumor photothermal-catalytic therapy. Chem Mater 31: 6174-6186, 2019.
3. Roper J, Tammela T, Cetinbas NM, Akkad A, Roghanian A, Rickelt S, Almeqdadi M, Wu K, Oberli MA, Sanchez-Rivera FJ, *et al*: In vivo genome editing and organoid transplantation models of colorectal cancer and metastasis. Nat Biotechnol 35: 569-576, 2017.
4. Vasaikar S, Huang C, Wang X, Petyuk VA, Savage SR, Wen B, Dou Y, Zhang Y, Shi Z, Arshad OA, *et al*: Clinical proteomic tumor analysis, proteogenomic analysis of human colon cancer reveals new therapeutic opportunities. Cell 177: 1035-1049, 2019.
5. Araghi M, Soerjomataram I, Jenkins M, Brierley J, Morris E, Bray F and Arnold M: Global trends in colorectal cancer mortality: Projections to the year 2035. Int J Cancer 144: 2992-3000, 2019.
6. Feletto E, Yu XQ, Lew JB, St John DJB, Jenkins MA, Macrae FA, Mahady SE and Canfell K: Trends in colon and rectal cancer incidence in australia from 1982 to 2014: Analysis of data on over 375,000 cases. Cancer Epidemiol Biomarkers Prev 28: 83-90, 2019.
7. MacKay JA, Chen M, McDaniel JR, Liu W, Simnick AJ and Chilkoti A: Self-assembling chimeric polypeptide-doxorubicin conjugate nanoparticles that abolish tumours after a single injection. Nat Mater 8: 993-999, 2009.
8. Xu L, Gordon R, Farmer R, Pattanayak A, Binkowski A, Huang X, Avram M, Krishna S, Voll E, Pavese J, *et al*: Precision therapeutic targeting of human cancer cell motility. Nat Commun 9: 2454, 2018.
9. Keklikoglou I, Cianciaruso C, Guc E, Squadrito ML, Spring LM, Tazzyman S, Lambein L, Poissonnier A, Ferraro GB, Baer C, *et al*: Chemotherapy elicits pro-metastatic extracellular vesicles in breast cancer models. Nat Cell Biol 21: 190-202, 2019.
10. Park NH, Cheng W, Lai F, Yang C, Florez de Sessions P, Periaswamy B, Wenhan Chu C, Bianco S, Liu S, Venkataraman S, *et al*: Addressing drug resistance in cancer with macromolecular chemotherapeutic agents. J Am Chem Soc 140: 4244-4252, 2018.
11. Baskar R, Lee KA, Yeo R and Yeoh KW: Cancer and radiation therapy: Current advances and future directions. Int J Med Sci 9: 193-199, 2012.
12. Huang Z, Wang Y, Yao D, Wu J, Hu Y and Yuan A: Nanoscale coordination polymers induce immunogenic cell death by amplifying radiation therapy mediated oxidative stress. Nat Commun 12: 145, 2021.
13. Moding EJ, Kastan MB and Kirsch DG: Strategies for optimizing the response of cancer and normal tissues to radiation. Nat Rev Drug Discov 12: 526-542, 2013.
14. Song G, Cheng L, Chao Y, Yang K and Liu Z: Emerging nanotechnology and advanced materials for cancer radiation therapy. Adv Mater: Jun 23, 2017 (Epub ahead of print).
15. Zhang S, Liu X, Bawa-Khalfe T, Lu LS, Lyu YL, Liu LF and Yeh ET: Identification of the molecular basis of doxorubicin-induced cardiotoxicity. Nat Med 18: 1639-1642, 2012.
16. Zhu AX, Rosmorduc O, Evans TR, Ross PJ, Santoro A, Carrilho FJ, Bruix J, Qin S, Thuluvath PJ, Llovet JM, *et al*: SEARCH: A phase III, randomized, double-blind, placebo-controlled trial of sorafenib plus erlotinib in patients with advanced hepatocellular carcinoma. J Clin Oncol 33: 559-566, 2015.
17. Breglio AM, Rusheen AE, Shide ED, Fernandez KA, Spielbauer KK, McLachlin KM, Hall MD, Amable L and Cunningham LL: Cisplatin is retained in the cochlea indefinitely following chemotherapy. Nat Commun 8: 1654, 2017.
18. Sara JD, Kaur J, Khodadadi R, Rehman M, Lobo R, Chakrabarti S, Herrmann J, Lerman A and Grothey A: 5-fluorouracil and cardiotoxicity: A review. Ther Adv Med Oncol 10: 1758835918780140, 2018.
19. Banik K, Ranaware AM, Harsha C, Nitesh T, Girisa S, Deshpande V, Fan L, Nalawade SP, Sethi G and Kunnumakkara AB: Piceatannol: A natural stilbene for the prevention and treatment of cancer. Pharmacol Res 153: 104635, 2020.
20. Ko HS, Lee HJ, Kim SH and Lee EO: Piceatannol suppresses breast cancer cell invasion through the inhibition of MMP-9: Involvement of PI3K/AKT and NF-κB pathways. J Agric Food Chem 60: 4083-4089, 2012.
21. Lee YM, Lim DY, Cho HJ, Seon MR, Kim JK, Lee BY and Park JH: Piceatannol, a natural stilbene from grapes, induces G1 cell cycle arrest in androgen-insensitive DU145 human prostate cancer cells via the inhibition of CDK activity. Cancer Lett 285: 166-173, 2009.
22. Xu Q, Fu Q, Li Z, Liu H, Wang Y, Lin X, He R, Zhang X, Ju Z, Campisi J, *et al*: The flavonoid procyanidin C1 has senotherapeutic activity and increases lifespan in mice. Nat Metab 3: 1706-1726, 2021.
23. Zhang L, Wang S, Liu Z, Zhang L, Wang S and Wang B: Procyanidin, a kind of biological flavonoid, induces protective anti-tumor immunity and protects mice from lethal B16F10 challenge. Int Immunopharmacol 47: 251-258, 2017.
24. Shang XJ, Yao G, Ge JP, Sun Y, Teng WH and Huang YF: Procyanidin induces apoptosis and necrosis of prostate cancer cell line PC-3 in a mitochondrion-dependent manner. J Androl 30: 122-126, 2009.
25. Lei Y, Ren X, Chen J, Liu D and Ruan J: Protective effects of grape seed-derived procyanidin extract against carrageenan-induced abacterial prostatitis in rats. J Funct Foods 7: 416-424, 2014.
26. Li S, Kodama EN, Inoue Y, Tani H, Matsuura Y, Zhang J, Tanaka T and Hattori T: Procyanidin B1 purified from Cinnamomi cortex suppresses hepatitis C virus replication. Antivir Chem Chemother 20: 239-248, 2010.
27. Na W, Ma B, Shi S, Chen Y, Zhang H, Zhan Y and An H: Procyanidin B1, a novel and specific inhibitor of Kv10.1 channel, suppresses the evolution of hepatoma. Biochem Pharmacol 178: 114089, 2020.
28. Koteswari LL, Kumari S, Kumar AB and Malla RR: A comparative anticancer study on procyanidin C1 against receptor positive and receptor negative breast cancer. Nat Prod Res 34: 3267-3274, 2020.
29. Lee Y: Cancer chemopreventive potential of procyanidin. Toxicol Res 33: 273-282, 2017.
30. Okamoto S, Ishihara S, Okamoto T, Doi S, Harui K, Higashino Y, Kawasaki T, Nakajima N and Saito A: Inhibitory activity of synthesized acetylated Procyanidin B1 analogs against HeLa S3 cells proliferation. Molecules 19: 1775-1785, 2014.
31. Mao JT, Xue B, Smoake J, Lu QY, Park H, Henning SM, Burns W, Bernabei A, Elashoff D, Serio KJ and Massie L: MicroRNA-19a/b mediates grape seed procyanidin extract-induced anti-neoplastic effects against lung cancer. J Nutr Biochem 34: 118-125, 2016.
32. Livak KJ and Schmittgen TD: Analysis of relative gene expression data using real-time quantitative PCR and the 2(-Delta Delta C(T)) method. Methods 25: 402-408, 2001.
33. Cagel M, Grotz E, Bernabeu E, Moretton MA and Chiappetta DA: Doxorubicin: Nanotechnological overviews from bench to bedside. Drug Discov Today 22: 270-281, 2017.
34. Tacar O, Sriamornsak P and Dass CR: Doxorubicin: An update on anticancer molecular action, toxicity and novel drug delivery systems. J Pharm Pharmacol 65: 157-170, 2013.
35. Ghosh P, Tiwari H, Lakkakula J, Roy A, Emran TB, Rashid S, Alghamdi S, Rajab BS, Almehmadi M, Allahyani M, *et al*: A decade's worth of impact: Dox loaded liposomes in anticancer activity. Mater Today Adv 16: 100313, 2022.
36. van Pelt-Sprangers MJ, Geijteman EC, Alsma J, Boere IA, Mathijssen RH and Schuit SC: Oromandibular dystonia: A serious side effect of capecitabine. BMC Cancer 15: 115, 2015.
37. James E, Podoltsev N, Salehi E, Curtis BR and Saif MW: Oxaliplatin-induced immune thrombocytopenia: Another cumulative dose-dependent side effect? Clin Colorectal Cancer 8: 220-224, 2009.
38. Zhao J, Zhang X, Cui X, Wang D, Zhang B and Ban L: Loss of fingerprints as a side effect of capecitabine therapy: Case report and literature review. Oncol Res 28: 103-106, 2020.